OPTOELECTRONICS AND ADVANCED MATERIALS – RAPID COMMUNICATIONS Vol. 12, No. 5-6, May-June 2018, p. 327 - 331

Study of band offset at ZnS/Cu_2ZnIVS_4(IV=Si,Ge,Sn) heterointerfaces

W. BAO[a,*], F. Y. QIU[a], S. BAI[b], Y. LI[a], D. M. CHEN[a]
[a] *College of New Energy, Bohai University, Jinzhou 121013, China*
[b] *College of Engineering, Bohai University, Jinzhou 121013, China*

Electrical transport properties of heterojunction solar cells are greatly influenced by the band offsets at the heterointerface. In this research, the band offsets of ZnS/Cu_2ZnIVS_4(IV=Si,Ge,Sn) heterointerfaces were studied by first-principles calculation method and their heterojunction solar cells were simulated by AMPS simulator. Band offset of ZnS/Cu_2ZnSiS_4 was observed to be type II heterointerface, with a cliff-like conduction band offset. ZnS/Cu_2ZnGeS_4 and ZnS/Cu_2ZnSnS_4 were demonstrated to be type I heterointerface with the large conduction band spike (0.7eV and 1.4eV, respectively), caused very little short circuit current densities.

(Received June 21, 2017; accepted June 7, 2018)

Keywords: Cu_2ZnIVS_4(IV=Si,Ge,Sn), Heterointerface, Band offset, Solar cell

1. Introduction

Cu_2ZnIVS_4(IV=Si,Ge,Sn) and their mixed cation alloys have attracted special attention for their potential applications in photovoltaic and optoelectronics [1-5]. For example, Cu_2ZnSnS_4(CZTS) is an excellent material as solar cell absorber since it contains abundant and nontoxic elements and has a 1.5 eV of band gap energy and large absorption coefficient in the order of 10^4 cm^{-1} [6,7]. Up to now, CZTS-based thin film solar cells with efficiency over 8.4% have already been fabricated [8]. The obtained results increase the interest in other Cu_2-II-IV-VI_4 series of quaternary chalcogenide semiconductors, including Cu_2ZnSiS_4 and Cu_2ZnGeS_4 with abundant and nontoxic component elements. Thus they could be considered as potential wide gap materials for photovoltaic applications.

Plenty of researches have been conducted on compounds Cu_2ZnIVS_4(IV=Si,Ge,Sn) and their mixed-cation alloys. The structural and electronic properties of Cu_2ZnIVS_4(IV=Si,Ge,Sn) have been studied by both theoretical and experimental means [9-14]. The phase stability and electronic structure of $Cu_2ZnSnSe_4$, $Cu_2ZnGeSe_4$ and $Cu_2ZnSiSe_4$ are theoretically evaluated. The investigations show that the kesterite phase is more stable than the stannite and wurtz-stannite phases [15,16]. About their mixed-cation alloys, it has been reported that $Cu_2Zn(Ge,Sn)(S,Se)_4$ compounds have good photovoltaic performance. It is noteworthy that the band graded $Cu_2Zn(Ge,Sn)(S,Se)_4$ films have improved the conversion efficiency up to 9.8% [5,17].

Electrical transport properties of heterojunction solar cells are greatly influenced by the band offsets at the heterointerface. According to the difference of the band gaps across the interface, they are divided into the valence band and the conduction band offsets. These offsets may dramatically influence both photo-current and dark current of the heterojunction solar cells. In Cu_2ZnIVS_4(IV=Si,Ge,Sn) three compounds, the energy level of the valence band maximum (VBM) do not change so much while that of the conduction band minimum (CBM) increase significantly with the atomic number of the group IV cations [15,16]. Therefore, in this study, in order to obtain an appropriate band discontinuity between window and absorber layer, we select the little lattice mismatch of ZnS as window layer to calculate and analyze the band offsets at ZnS/Cu_2ZnIVS_4 heterointerface with different cations of group IV(IV=Si,Ge,Sn). The calculation of band offset was performed on the basis of the first-principles, density-functional theory (DFT) and pseudopotential method. The effect of band offset quantitatively explained by using device modeling and simulation method.

2. Calculation

Cu_2ZnIVS_4(IV=Si,Ge,Sn) compounds crystallize in the kesterite structure and ZnS crystallizes in the zinc-blende structurein this study. The calculation of density of states was performed on the basis of the first-principles, DFT and pseudopotential method, using the PHASE code developed by Institute of Industrial Science, University Tokyo [18]. We employed the generalized gradient approximation for the exchange-correlation interaction

[19], with valence electron configurations of S ($3s^2$, $3p^4$), Cu ($3d^{10}$, $4s^1$), Zn ($3d^{10}$,$4s^2$), Si ($3s^2$,$3p^2$), Ge ($4s^2$,$4p^2$) and Sn ($4d^{10}$, $5s^2$,$5p^2$). For a given atomic arrangement, the lattice constants and atom positions were optimized to minimize the total energy.

We first obtained the energy level differences between the reference core levels (take S-3s, Zn-3d, Si-3s, Ge-4s and Sn-4das reference core levels in the pseudopotential calculation method) and the VBM from the band structures of ZnS and Cu_2ZnIVS_4(IV=Si, Ge and Sn). Then, the core level difference was obtained from the band structure of the (001) crystal plane in ZnS/Cu_2ZnIVS_4(IV=Si, Ge, Sn) superlattice. The valence band offset ΔE_V and conduction band offset ΔE_C were obtained as follows [20,21]:

$$\Delta E_v = \Delta E^1_{VBM-core} - \Delta E^2_{VBM-core} - \Delta E^{2/1}_{Core} \quad (1)$$

$$\Delta E_c = \left|\Delta E_g - \Delta E_v\right| \quad (2)$$

where $\Delta E^1_{VBM-core}$ ($\Delta E^2_{VBM-core}$) is the energy level difference between the reference core levels and the VBM for the ZnS and Cu_2ZnIVS_4(IV=Si, Ge and Sn) bulk, and $\Delta E^{2/1}_{VBM-core}$ is the difference of the core level energies in the ZnS/Cu_2ZnIVS_4 supercells. This equation was based on the idea that the energy difference between the core level and the VBM in the respective bulk material is conserved in the heterostructure. ΔE_g is the band gap difference between ZnS and Cu_2ZnIVS_4(IV=Si, Ge and Sn).

3. Results and discussion

The total density of states for kesterite structure of Cu_2ZnIVS_4(IV=Si, Ge and Sn) are calculated as shown in Fig. 1, and the zero point energy is taken as VBM. The band gaps are 1.33, 0.38 and 0.04 eV for Cu_2ZnSiS_4, Cu_2ZnGeS_4 and Cu_2ZnSnS_4, respectively, which decreases with the group VI atoms changing from Si, Ge to Sn in turn. Due to the limitation of DFT, these calculated band gaps are smaller than the experimental values (3.0, 2.1 and 1.5 eV [22, 23]). But it has less effect on investigating the electronic structure in the present work. Since the band gap is generally underestimated in the calculation based on the generalized gradient approximation, the band gap energies employed experimental values. The VBM of these compounds primarily consist of S-3p and Cu-3d orbitals, the CBM is the antibonding states of the hybridization between the group IV(Sn,Ge,Si)-s orbitals and S-3p orbitals [24].

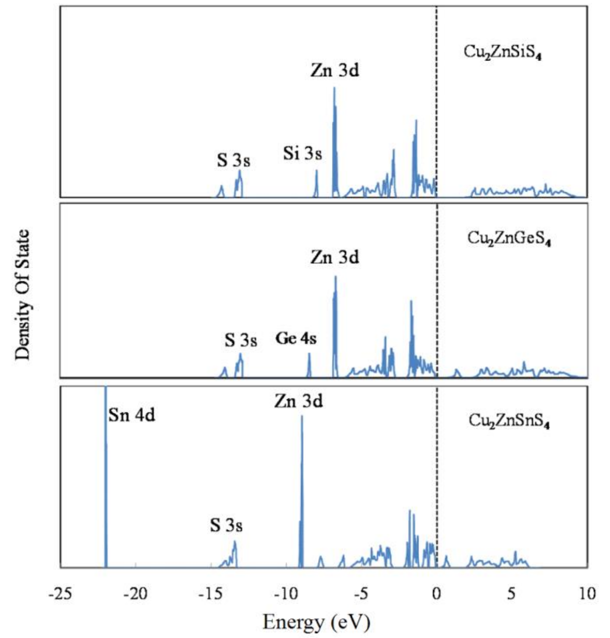

Fig. 1. Density of states for Cu_2ZnIVS_4(IV=Si, Ge and Sn)

The calculated band offsets at ZnS/Cu_2ZnIVS_4(IV=Si,Ge,Sn) heterointerfaces are shown in Fig. 2. The VBM of Cu_2ZnIVS_4(IV=Si,Ge,Sn) is higher than that of ZnS, while the valence band offsets of the three heterointerfaces are almost the same, with values of 0.8, 0.9 and 1.0 eV, respectively. The conduction band offsets increase significantly from ZnS/Cu_2ZnSnS_4, ZnS/Cu_2ZnGeS_4 to ZnS/Cu_2ZnSiS_4 heterointerfaces in sequence. It can be primarily attributed to the up shift of the conduction band, with a much smaller contribution of the downshift of the valence band for Cu_2ZnSnS_4, Cu_2ZnGeS_4 to Cu_2ZnSiS_4. The reason for the similar valence band offsets is that the approximate VBM of these compounds primarily consists of S-3p and Cu-3d orbitals [24]. Therefore, substitution of Sn by Ge or Si does not affect the VBM energy levels significantly. On the other hand, the lowest conduction band is the antibonding states of the hybridization between the group IV (Sn,Ge,Si)-s orbitals and S-3p orbitals. In comparison with Cu_2ZnGeS_4, the antibonding CBM of Cu_2ZnSnS_4has lower energy due to the larger bond length of Sn-S than that of Ge-S. And it is easy to understand the lower CBM of Cu_2ZnGeS_4 than Cu_2ZnSiS_4 in the same way.

ΔE_v obtained in this work (0.9 eV for the ZnS/Cu_2ZnGeS_4 superlattices) is smaller than the result of the previous theoretical work by Chen et al. (ΔE_v= 1.14eV). It was explained by the difference of band energies caused by the different strain effect conditions, owning to the exchange of interaction among the atomic orbitals under compressive or tensile strain (with exchange in the interatomic spacing). In this work, the average value

of lattice constants for ZnS and Cu_2ZnIVS_4(IV=Si,Ge,Sn) bulk materials was used for the lattice constant along the heterointerface. The lattice spacing in the perpendicular direction was assumed to be the same as in the respective bulk material. In their calculation [24], the band offset was obtained in the condition of a full relaxed interface, where each component had its own equilibrium lattice parameter. The core level difference $\Delta E^{2/1}_{Core}$ between the two semiconductors was obtained from the calculation for the ZnS/Cu_2ZnGeS_4 superlattices with (001) orientation. Thus the result of band offset at ZnS/Cu_2ZnGeS_4 is different from the reference [24].

As shown in Fig. 2, ZnS/Cu_2ZnSiS_4 band alignment is of type II heterointerface, the conduction band offset is 0.3eV which CBM of Cu_2ZnSiS_4 is higher than that of ZnS. There is no barrier for the flow of photogenerated electrons from Cu_2ZnSiS_4 to ZnS. Therefore, the quantum efficiency can be high. The band alignments of ZnS/Cu_2ZnGeS_4 and ZnS/Cu_2ZnSnS_4 are of type I heterointerfaces, where the CBM of Cu_2ZnGeS_4 and Cu_2ZnSnS_4 are both lower than that of ZnS, with values of 0.7eV and 1.4eV, respectively. The conduction band offsets form a barrier for the photoexcited electrons crossing the interface. Heights of these barriers are larger than 0.4 eV, which will considerably reduce the photocurrent [25].

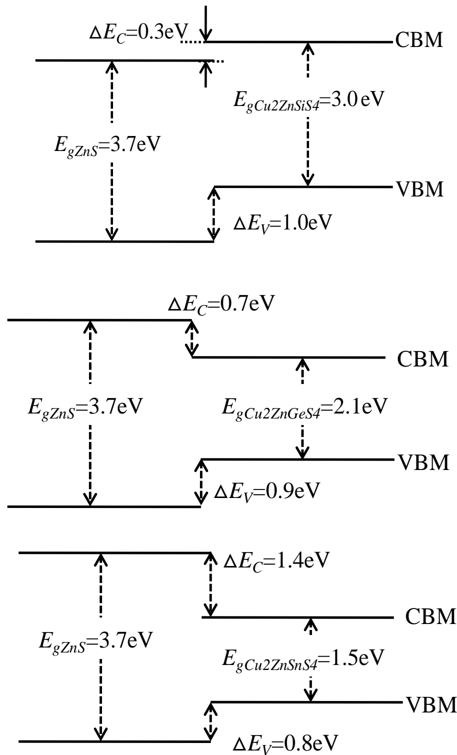

Fig. 2. Band offsets at ZnS/Cu_2ZnIVS_4(IV=Si,Ge,Sn) heterointerfaces

However, it has only been explained qualitatively the effect of the conduction band offset between window and absorber on performance of Cu_2ZnIVS_4(IV=Si,Ge,Sn) solar cells. The device modeling and simulation were conducted to explain the effect of conduction band offset quantitatively. The energy-bands were simulated using the AMPS device modeling software package [26]. The parameters used for simulations of ZnS/Cu_2ZnIVS_4(IV=Si,Ge,Sn) solar cells are summarized in the following Table 1. The conduction band offset of ZnS/Cu_2ZnIVS_4 layers was adjusted by changing the electron affinity of absorber layer and realistic doping levels are 10^{18} cm^{-3} and 10^{17} cm^{-3} for the n-ZnS and p-Cu_2ZnIVS_4(IV=Si,Ge,Sn).

Fig. 3 displays the calculated band alignment of ZnS/Cu_2ZnIVS_4(IV=Si,Ge,Sn) heterojunction under equilibrium conditions. The simulations demonstrated the ZnS/Cu_2ZnSiS_4 is the cliff-like conduction band offset of heterointerface, as showed in Fig. 3(a). There is no barrier for the charge transfer at the heterointerface, but the output voltage is expected to be small for a type II interface in general. *I-V* measurements performed on ZnS/Cu_2ZnSiS_4 heterojunction device confirmed this notion, exhibiting short-circuit current densities of 26.2 mA/cm^2 under simulated AM1.5 1-Sun illumination. However, the devices consistently demonstrated open circuit voltage of 60.0 mV, indicating the output voltage was reduced by increasing the recombination rate of the majority carriers at the interface. As shown in Fig. 3(b) and Fig. 3(c), there are existences of a large conduction-band spike at the ZnS/Cu_2ZnGeS_4 and ZnS/Cu_2ZnSnS_4 interfaces due to the calculated band offset. *I-V* measurements indicated the large conduction band spike inhibited the charge transport across the heterojunction devices, which resulted in short-circuit current densities of 0.6 mA/cm^2 and 0.4 mA/cm^2, respectively. The devices demonstrated open circuit voltage of 277.5 mV and 549.7 mV, which were relatively higher than type II interface of ZnS/Cu_2ZnSiS_4.

Table 1. The parameters used for simulations of ZnS/Cu_2ZnIVS_4(IV=Si,Ge,Sn) solar cell

Parameters	ZnS	Cu_2ZnSiS_4 (Cu_2ZnGeS_4, Cu_2ZnSnS_4)
Layers thickness (nm)	200	3000
Dielectric constant (relative)	10	7.5[1] (6.8[2], 7.0[3])
Electron affinity (eV)	2.7	2.4 (3.4, 4.1)
Band-gap (eV)	3.7	3.0 (2.1[2], 1.5)
Effective conduction band density (cm^{-3})	2.2×10^{18}	2.2×10^{18}
Effective valence band density (cm^{-3})	1.8×10^{19}	1.8×10^{19}
Electron thermal velocity (cm/s)	1.0×10^{7}	1.0×10^{7}
Electron thermal velocity (cm/s)	1.0×10^{7}	1.0×10^{7}
Electron mobility ($cm^2v^{-1}s^{-1}$)	100	60
Hole mobility ($cm^2v^{-1}s^{-1}$)	25	20
Doping concentration of acceptors (cm^{-3})	0	10^{17}
Doping concentration of donators (cm^{-3})	10^{18}	0

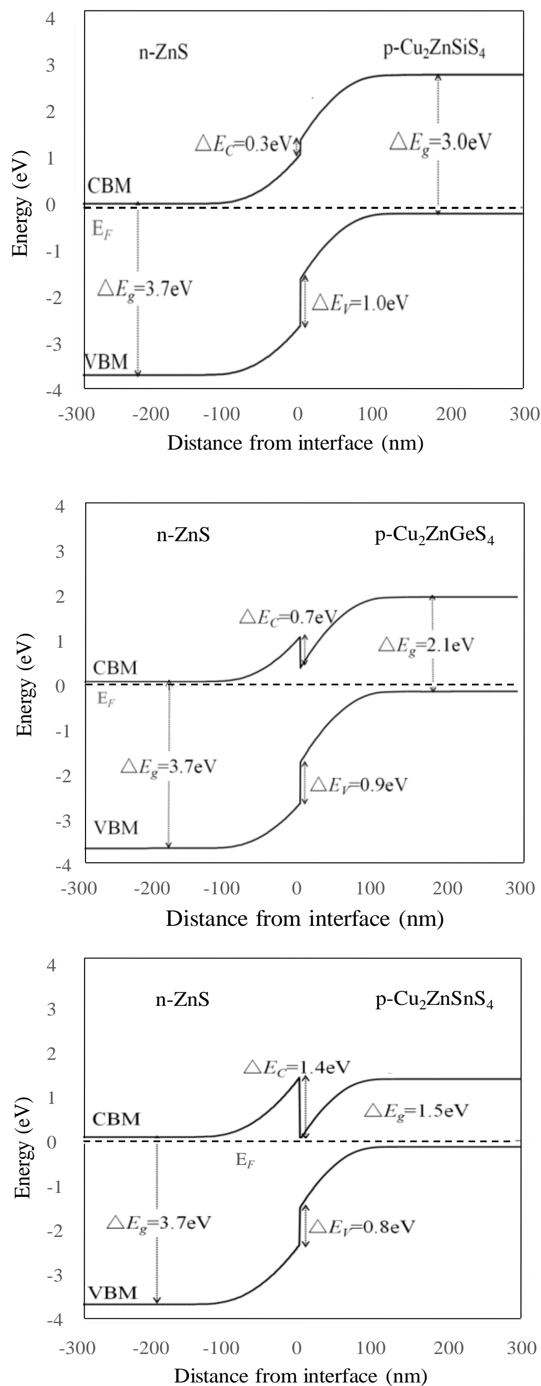

Fig. 3. Energy band offsets for ZnS/Cu_2ZnIVS_4(IV=Si,Ge,Sn) heterointerfaces that was calculated given the first principles calculated ΔE_V and given the assumed doping level are $1\times10^{18} cm^{-3}$ and $1\times10^{17} cm^{-3}$ for n-ZnS and p-Cu_2ZnIVS_4 (IV=Si,Ge,Sn) layers

The obtained short-circuit current densities of ZnS/Cu_2ZnSnS_4 solar cells in this work (0.4 mA/cm^2) are significantly smaller than the previous experimental work (12.16 mA/cm^2) [27]. It was mainly because that, some oxygen ions of the intrinsic ZnO layer (i-ZnO) can diffuse into the ZnS layer to form Zn(O,S) during the device fabrication, which reduced the positive conduction band offset at the Zn(O,S)/CZTS interface [28]. The reduced positive conduction band offset led to a small resistance barrier for electrons to flow. On the other hand, the obtained bigger open circuit voltage in this work (549.7 mV) higher than the experimental work (311 mV) can be explained by the high density of defects at ZnS/CZTS interface [29]. Therefore, the theoretical results obtained here were more in consistent with the observed solar cell properties.

According to the above results, it is considered that the suitable conduction band offset and higher efficiency can be obtained by controlling the Si composition in $Cu_2Zn(Si,Sn)S_4$ alloys. The calculation showed that Si were well alloyed with Sn in $Cu_2Zn(Si,Sn)S_4$ alloy [30]. The band gaps were tuned by substitution of Si for Sn and increased with Si content. The $Cu_2Zn(Si,Sn)S_4$ alloys tuned by the fabricated band-gap can have good photovoltaic performance, thus able to achieve higher conversion efficiency in $ZnS/Cu_2Zn(Si,Sn)S_4$ solar cells.

4. Conclusions

In this work, we calculated the band offsets at ZnS/Cu_2ZnIVS_4(IV=Si,Ge,Sn) heterointerfaces by using the first-principles calculation method. The conduction band offsets decreased significantly from ZnS/Cu_2ZnSiS_4, ZnS/Cu_2ZnGeS_4 to ZnS/Cu_2ZnSnS_4 heterointerfaces. The ZnS/Cu_2ZnSiS_4 band alignment was of type II heterointerface with a 0.3eV of conduction band offset, during which the conduction CBM of Cu_2ZnSiS_4 was higher than that of ZnS. Nevertheless, ZnS/Cu_2ZnGeS_4 and ZnS/Cu_2ZnSnS_4 were demonstrated to be type I heterointerface. The CBM of Cu_2ZnGeS_4 and Cu_2ZnSnS_4 were both lower than that of ZnS and their conduction band offsets were 0.7eV and 1.4eV, respectively. The effect of conduction band offsets was quantitatively explained by employing device modeling and simulation method. It was found that the cliff-like conduction band offset of ZnS/Cu_2ZnSiS_4 heterointerface exhibitied a short-circuit current density of 26.2 mA/cm^2 and an open circuit voltage of 60.0 mV under simulated AM1.5 1-Sun illumination. While the large conduction band spike of ZnS/Cu_2ZnGeS_4 and ZnS/Cu_2ZnSnS_4 heterojunction devices, showed a short-circuit current densities of 0.6 mA/cm^2 and 0.4 mA/cm^2 and open circuit voltage of 277.5mV and 549.7 mV, respectively.

Acknowledgment

This work was supported by the Special Funds of the National Natural Science Foundation of China, 11547226 11547180 and 11747118.

References

[1] H. Katagiri, Thin Solid Films **480**, 426 (2005).
[2] K. Wang, O. Gunawan, T. Todorov, B. Shin, S. J. Chey, N. A. Bojarczuk, D. Mitzi, S. Guha, Appl. Phys. Lett. **97**, 143508 (2010).
[3] M. Hamdi, A. Oueslati, A. Lafond, C. Guillot-Deudon, F. Hlel, J. Alloy. Compd. **674**, 73 (2016).
[4] M. Singh, T. R. Rana, J. H. Kim, J. Alloy. Compd. **675**, 370 (2016).
[5] I. Kim, K. Kim, Y. Oh, et al., Chem. Mater. **26**, 3957 (2014).
[6] A. Ennaoui, M. Lux-Steiner, A. Weber, D. Abou-ras, I. Kotschau, H. W. Schock, R. Shurr, A. Holzing, S. Jost, R. Hock, T. VoB, J. Schulze, A. Kirbs, Thin Solid Films **517**, 2511 (2009).
[7] H. Katagiri, K. Jimbo, S. Yamada, T. Kamimura, W. S. Maw, T. Fukano, T. Ito, T. Motohiro, Appl. Phys. Express **1**, 041201 (2008).
[8] B. Shin, O. Gunawan, Y. Zhu, N.-A.Bojarczuk, S. Jay Chey, S. Guha, Prog. Photovoltaics. **21**, 72 (2013).
[9] X. Zhang, D. Chen, K. Deng, R. Lu, J. Alloy. Compd. **656**, 196 (2016).
[10] K. A. Rosmus, C. D. Brunetta, M. N. Srnec, B. Karuppannan, J. A. Aitken, Z. Anorg. Allg. Chem. **638**, 2578 (2012).
[11] H. Matsushita, T. Ichikawa, A. Katsui, J. Mater. Sci. **40**, 2003 (2005).
[12] M. León, S. Levcenko, R. Serna, G. Gurieva, A. Nateprov, J. M. Merino, E. J. Friedrich, U. Fillat, S. Schorr, E. Arushanov, J. Appl. Phys. **108**, 093502 (2010).
[13] O. V. Parasyuk, L. V. Piskach, Y. E. Romanyuk, I. D. Olekseyuk, V. I. Zaremba, V. I. Pekhnyo, J. Alloys Compd. **397**, 85 (2005).
[14] S. Chen, X. G. Gong, A. Walsh, S.-H. Wei, Appl. Phys. Lett. **94**, 041903 (2009).
[15] Q. Shu, J. H. Yang, S. Chen, B. Huang, H. Xiang, X. G. Gong, S. H. Wei, Phys. Rev. B: Condens. Matter. **87**, 269 (2013).
[16] S. Nakamura, T. Maeda, T. Wada, Jpn. J. Appl. Phys. **49**, 121203 (2010).
[17] C. J. Hages, S. Levcenco, C. K. Miskin, J. H. Alsmeier, D. AbouRas, R. G. Wilks, M. Bar, T. Unold, R. Agrawal, Process. Prog. Photovoltaics Res. Appl. **23**, 376 (2013).
[18] http://www.ciss.iis.u-tokyo.ac.jp/rss21/en/index.html
[19] J. P. Perdew, K. Burke, M. Ernzerhof, Phys. Rev. Lett. **77**, 3865 (1996).
[20] A. J. Nelson, C. R. Schwerdtfeger, S. H. Wei et. al., Appl. Phys. Lett. **62**, 2557 (1993).
[21] S. H. Wei, A. Zunger, Appl. Phys. Lett. **63**, 2549 (1993).
[22] G. Q. Yao, H. S. Shen, E. D. Honig, R. Kershaw, K. Dwight, A. Wold, Solid State Ionics **24**, 249 (1987).
[23] D. Chen, N. M. Ravindra, J. Alloy. Compd. **579**, 468 (2013).
[24] S. Chen, X. G. Gong, A. Walsh, S. H. Wei, Phys. Rev. B. **79**, 165211 (2009).
[25] T. Minemoto, T. Matsui, H. Takakura, Y. Hamakawa, T. Negami, Y. Hashimoto, T. Uenoyama, M. Kitagawa, Sol. Energy Mater. Sol. Cells. **67,** 83(2001).
[26] https://wiki.engr.illinois.edu/display/solarcellsim.
[27] J. Kim, C. Park, S. M. Pawar, et al., Thin Solid Films, **566**, 88 (2014).
[28] T. Ericon, J. J. Scragg, A. Hultqvist, J. T. Watjen, P. Szaniawski, T. Torndahl, C. Platzer-Bjorkman, IEEE J. Photovoltaics **4**, 465 (2013).
[29] M. M. Islam, S. Ishizuka, A. Yamada, K. Sakurai, S. Niki, T. Sakurai, K. Akimoto, Sol. Energy Mater. Sol. Cells.**93**, 970 (2009).
[30] Q. Shu, J. H. Yang, S. Chen, B. Huang, H. Xiang, X. G. Gong, S. H. Wei, Phys. Rev. B. **87**, 115208 (2013).

*Corresponding author: baowujisgl@bhu.edu.cn, baowjsgl@126.com